THESIS FOR THE DEGREE OF LICENTIATE OF ENGINEERING

Influence of the Processing Atmosphere on Binder Jetting of Stainless Steel: From Printing to Sintering

KAI ZISSEL

CHALMERS

Department of Industrial and Materials Science

CHALMERS UNIVERSITY OF TECHNOLOGY

Gothenburg, Sweden 2024

Influence of the Processing Atmosphere on Binder Jetting of Stainless Steel: From Printing to Sintering
KAI ZISSEL

Technical report no IMS-2024-6
Licentiate Thesis at Chalmers University of Technology
Department of Industrial and Materials Science
Chalmers University of Technology
SE-412 96 Gothenburg
Sweden
Telephone + 46 (0)31-772 1000

Printed by Chalmers Reproservice

Gothenburg, Sweden 2024

Influence of the Processing Atmosphere on Binder Jetting of Stainless Steel: From Printing to Sintering

KAI ZISSEL
Department of Industrial and Materials Science
Chalmers University of Technology

Abstract

Binder Jetting (BJT) is considered a promising Additive Manufacutring (AM) technology for the production of complex metal components due to its high productivity and cost efficiency compared to other AM technologies. The BJT technology is a multi-step process that consists of printing, curing, depowdering, debinding and sintering. Each process step includes individual process parameters. One crucial variable across each step is the processing atmosphere.

A robust process is a prerequisite for manufacturing consistent green parts. Printing in BJT is conducted at ambient temperature. The reusability of the metal powder is considered unproblematic since no oxidation is expected during printing. However, the impact of powder reuse and specifically curing on printing behavior has not been extensively studied in BJT. Therefore, the first part of this study investigated the influence of powder reuse on powder characteristics and printing results for 17-4 PH stainless steel. Furthermore, different curing atmospheres were compared. The green densities obtained after printing decreased from 4.71 g/cm^3 to 4.47 g/cm^3 after 20 build jobs, which correlated with an oxygen pickup of the powder during curing. In addition, the median particle size increased by ~1 µm after 20 build jobs. Curing in inert environments such as nitrogen (N_2) is shown as advantageous since oxidation of the powder is limited.

The debinding process aims to remove the binder efficiently without contaminating the material. Debinding can be conducted in air to utilize oxygen (O_2) for binder decomposition. The powder is, however, prone to oxidation at elevated debinding temperatures. Consequently, the decrease in the oxygen content in the debinding atmosphere at 300 °C for 2 h was studied. The results demonstrated that the carbon introduced by the binder can enhance oxide reduction by carbothermal reduction. Debinding in inert argon (Ar) resulted in low binder removal, but led to nearly complete oxygen removal after sintering. The formation of δ-ferrite was prohibited due to the high carbon content resulting in low sintered densities of ~88 %. Debinding in Ar + 1 vol.% O_2 reduced oxygen content by 46 % relative to the virgin powder. At the same time, high densities of ~98 % were obtained with no carbon pick-up after sintering. Debinding in processing atmospheres containing 3 vol.% O_2 to 20 vol.% O_2 allowed to remove the binder almost completely but increased the brown part brittleness. While oxygen reduction was measured from brown to sintered components, the oxidation caused during debinding was not sufficiently reversed by carbothermal reduction during sintering in an inert Ar atmosphere.

Keywords: Binder Jetting, Additive Manufacturing, Debinding, Sintering, Stainless Steel, 17-4 PH, Powder Reusability, Processing Atmosphere, Oxidation, Carbothermal Reduction

Preface

This Licentiate thesis is based on the research conducted at the Technology Center of Linde GmbH and the Department of Industrial and Materials Science at Chalmers University of Technology. The work presented in this thesis was performed between July 2021 and February 2024. The industrial supervisor was Pierre Forêt. The academic supervisor was professor Eduard Hryha.

The author acknowledges funding by the Federal Ministry of Research and Education (BMBF, Germany), for the project SINEWAVE (FKZ 03HY123A) within the Hydrogen Flagship Project H2Giga. This work was also conducted in the framework of the Centre for Additive Manufacturing – Metal (CAM^2), supported by the Swedish Governmental Agency of Innovation Systems (Vinnova).

The thesis includes an introductory part explaining the processing chain of Binder Jetting and briefly summarizing the role of the processing atmosphere for each step. The research focused on powder reuse and the optimization of the debinding atmosphere for a stainless steel. Most of the work was summarized in the appended papers.

List of appended papers

Paper I: **Binder Jetting – Reusability of 17-4 PH Stainless Steel Powder**
Kai Zissel, Elena Bernardo Quejido, Tobias Deckers, Pierre Forêt, Eduard Hryha
WorldPM2022 Conference proceedings, 2022

Paper II: **Impact of oxygen content on debinding of binder jetted 17-4 PH stainless steel parts: Part I – Debinding**
Kai Zissel, Elena Bernardo Quejido, Pierre Forêt, Eduard Hryha
In Manuscript

Paper III: **Impact of oxygen content on debinding of binder jetted 17-4 PH stainless steel: Part II – Sintering**
Kai Zissel, Elena Bernardo Quejido, Pierre Forêt, Eduard Hryha
In Manuscript

Contribution to the appended papers

Paper I: The author planned the work together with co-authors and performed the major part of the experimental work. The author carried out the analysis of the results and wrote the paper in close cooperation with the co-authors.

Paper II: The author planned and was involved in the execution of the experimental work. The author carried out the analysis of the results and wrote the paper in close cooperation with the co-authors.

Paper III: The author planned and was involved in the execution of the experimental work. The author carried out the analysis of the results and wrote the paper in close cooperation with the co-authors.

Table of Contents

1 Introduction

Additive Manufacturing (AM) is a production technology for metals, which enables new and complex design structures that are not feasible with conventional manufacturing technologies such as casting, forging and machining. Further benefits include reduced material waste, topology optimization, part consolidation and rapid prototyping. The described advantages led to applications in diverse industries, especially aerospace and healthcare [1,2]. The widespread adoption of metal AM in more cost-driven industries such as automotive is hindered by the low productivity and high costs per part compared to conventional manufacturing technologies [3,4].

Binder Jetting (BJT) is an emerging AM technology that promises a more productive and cost-effective way of producing metal components compared to other AM technologies such as Powder Bed Fusion (PBF) [5]. The BJT printing is based on inkjet technology, where a liquid binder is deposited on spread layers of metal powders to glue the particles together. The layer-wise repetition results in a powder bed containing the so-called 'green' parts. After printing, the binder is typically hardened by a thermal process named curing. Once the binder is hardened, the green parts are separated from the loose powder bed. After the depowdering step, the green parts are debinded and sintered at high temperatures to gain a dense metal material. Accordingly, BJT of metals is classified as a multi-step process (BJT-MSt/M) [6].

Each step of the BJT process includes various process parameters that influence the outcome of the final component. One key variable encountered in every step along the process chain is the processing atmosphere, but its significance is often underestimated in the industry. Process repeatability is a prerequisite for serial production, where specified tolerances and material properties need to be fulfilled for technical applications. The cause-and-effect relationship between raw material, processing parameters and resulting material properties must be understood in detail. The processing atmosphere is especially important for curing, debinding and sintering, where the metal is subjected to heat. A tailored and well-controlled process atmosphere is required to ensure process robustness and improve material performance.

Structural parts of stainless steel are of major interest in binder-assisted powder processing including BJT [7]. One major challenge of BJT is the production of consistent green parts, which can be affected by powder reuse. To be cost-efficient and to reduce material waste, the powder used for printing needs to be reused. Differences in green parts will be amplified during debinding and sintering. As printing is typically conducted in ambient conditions at room temperature (RT), the potential of powder reuse in BJT is considered generally high.

Studies on powder reuse and its influence on powder characteristics and green part consistency are limited. The impact of the curing process on powder characteristics is typically not monitored even though the curing process is commonly conducted in

ambient air at elevated temperatures. Oxygen (O_2) in the atmosphere provides conditions for powder oxidation. A better understanding of potential powder degradation and its effect on printing results is vital. Consequently, the impact of curing in ambient air on powder reuse and degradation was analyzed in detail. The effect of different curing atmospheres on the metal powder was compared.

The final dimensions and material properties of BJT components are determined by the debinding and sintering parameters. A well-controlled debinding and sintering process is substantial to reach the required material properties for high-performance applications of stainless steels. The debinding process poses a challenge since complete binder removal and preservation of the metal powder quality need to be achieved simultaneously.

Efficient debinding at moderate temperatures can require oxygen, typically stemming from the air, to aid the decomposition of the binder. The powder is, however, prone to undesirable oxidation at typical debinding temperatures. Excessive powder oxidation hinders the densification during sintering [8]. Furthermore, elevated oxygen contents can be detrimental to the mechanical performance and corrosion resistance of sintered stainless steels [9,10]. Therefore, optimizing the debinding atmosphere by decreasing its oxygen content was investigated.

The research was conducted on 17-4 PH stainless steel, which is a popular material choice in BJT due to its unique combination of excellent mechanical performance and corrosion resistance. At first, this work investigated the reusability of 17-4 PH powder for 20 reuse cycles. In the next step, optimizing the debinding process by reducing the oxygen content in the debinding atmosphere was explored, followed by sintering in an inert Ar atmosphere.

1.1 Research objectives

The research objectives of this thesis study can be separated into two parts. In the first part, the research aimed at providing a more comprehensive understanding of how powder characteristics change over multiple reuse cycles. Moreover, the role of the curing atmosphere was investigated. The second objective was to achieve efficient binder removal and minimize powder oxidation by varying oxygen content in the debinding atmosphere. The chemical evolution from virgin powder to sintered part was closely compared. Hence, the two main research questions (RQ) addressed in this study are the following:

1. What is the influence of curing in ambient air on powder degradation and printing repeatability during BJT of 17-4 PH stainless steel?
2. What is the impact of decreasing oxygen in the processing atmosphere during debinding on 17-4 PH green part properties, sintering densification and material chemistry?

2 Metal Binder Jetting

Metal Binder Jetting comprises multiple subsequent manufacturing steps that are shown in Figure 1. The process can be divided into the production of a green part and the thermal treatment of the obtained green parts. The green part manufacturing includes printing, curing and depowdering. The thermal treatments are debinding and sintering, where a dense metal component is formed. In this chapter, a basic understanding of each manufacturing step along the process chain is given.

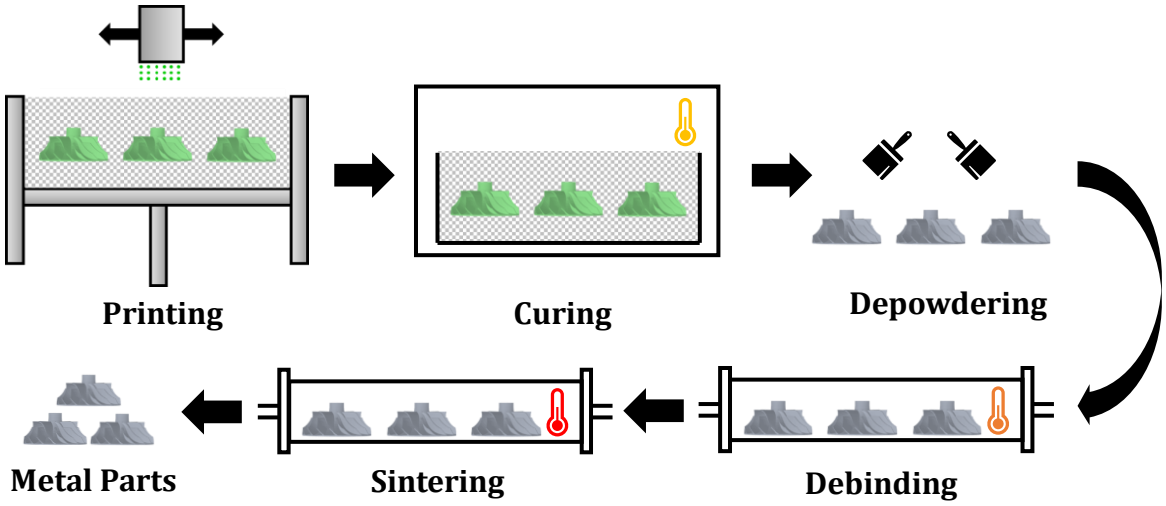

Figure 1: Manufacturing chain for Binder Jetting of metals.

2.1 Printing, Curing & Depowdering

The basic principle of BJT is based on a binder that glues metal particles together. The printing process starts with depositing a powder layer onto the build plate. The powder is typically compacted by a roller or blade to achieve a dense powder layer. Particle diameters are typically below 25 µm and the layer thickness usually range from 40 µm to 100 µm [11]. Afterward, binder droplets are jetted onto the powder layer by a printhead. The position of the binder is defined by the cross-section of the three-dimensional (3D) models at that specific layer height. After the jetting, an infrared (IR) heater or thermal energy can be applied to cure the binder depending on the machine and binder formulation. Subsequently, the build plate is lowered and the steps are repeated. This iterative printing process, which is sketched in Figure 2, results in the shaping of a 3D green part in the powder bed.

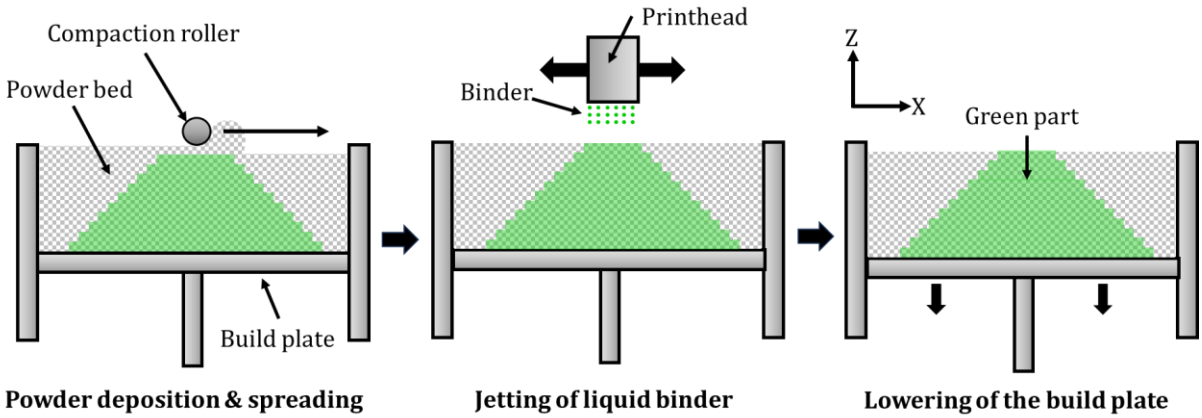

Figure 2: Illustration of the BJT printing process.

After printing, a heat treatment between 80 °C to 250 °C for several hours is usually performed to harden the binder and evaporate water and solvents. The curing process ensures sufficient strength so the printed parts can be removed from the surrounding powder bed. This step is known as depowdering. The obtained green part is a mixture of metal powder and hardened binder. The BJT printing process does not require support structures as the powder bed provides sufficient support.

2.2 Debinding

After printing, curing and depowdering, the green part is placed into a furnace for a thermal treatment up to 600 °C to remove the binder. This step is referred to as debinding. After the debinding process is completed, the component is called 'brown' part. The function of the binder is to keep the metal powder compact in the desired shape until the metal powder particles form metallurgical bonds at the onset of sintering.

Most BJT binders rely on a single thermal debinding step due to the relatively low binder content in contrast to other binder-based technologies that need a separate debinding step in a solvent [12]. Thermal debinding is preferred in the industry and is commonly combined into one step with the sintering process [11]. Heating leads to the expansion of the binder and slight swelling of the part. The binder can melt, migrate and fragment. Its decomposition products finally evaporate from the green part. Successful debinding is defined as the complete removal of the binder without damaging or contaminating the component [11]. The debinding process has to balance processing time and defect-free removal of the binder. The higher the heating rates that are applied, the more likely damage can occur such as blisters due to the increasing pressure generated by the debinding products. Cracks generated during debinding are often not observed until after sintering, which enlarges the cracks that can be mistaken to be formed during sintering [11].

The difficulty and time of the debinding process are closely tied to the binder formulation, the binder content, the green part size and the processing atmosphere. The debinding front migrates from the outside to the inside of the green part, which is illustrated in Figure 3 [11]. In the first stage of debinding, the binder removal penetrates continuously

into the green part with increasing transport distances for binder removal [11]. At the same time, the distances for the penetration of the processing atmosphere or catalytic agents increase [11]. A gradient of concentrations is formed from the surface to the core of the part.

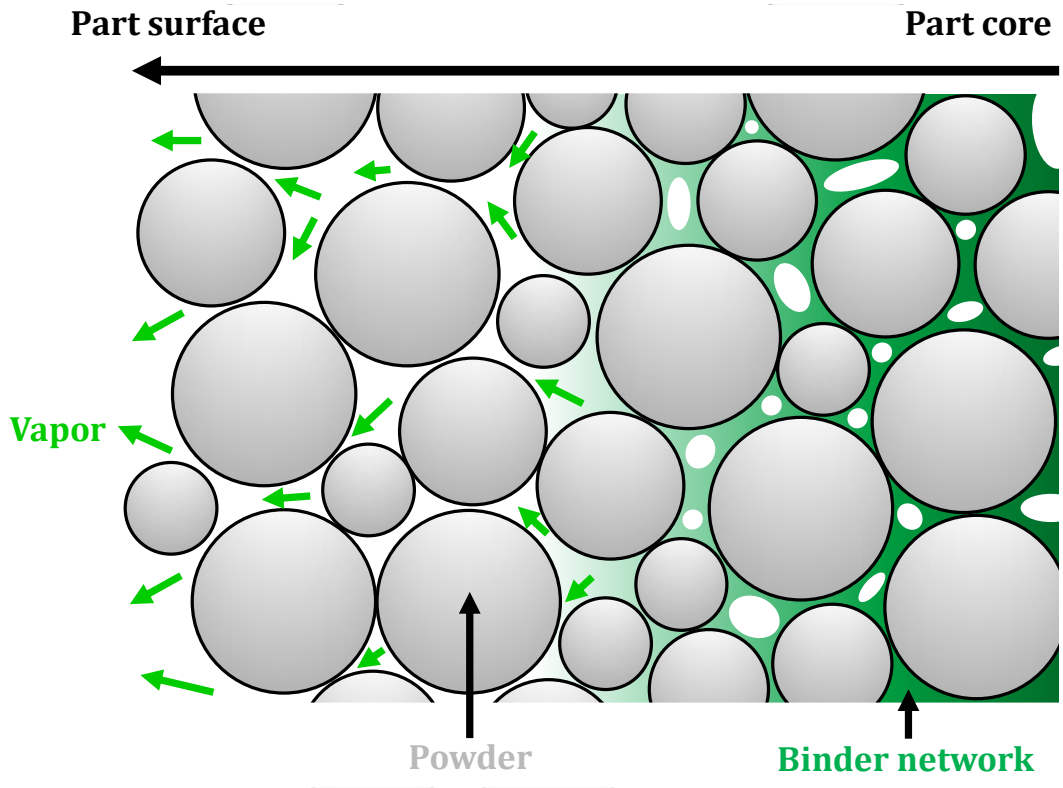

Figure 3: Schematic illustration of the thermal debinding process inside a green part.

The rate-controlling transport step is determined by molten binder flow in the pores, binder evaporation, or the permeation of vapor through the pores. In the beginning, the binder removal is controlled by heat penetration and binder melting. The binder vaporization inside the green part becomes the limiting step in the later stage of debinding [11]. This is not an issue for thin components. Thick parts possess a decreasing rate of binder removal over time.

As polymers are subjected to high temperatures, various reactions can take place [12]. While the binder can directly evaporate, it more commonly disintegrates into different hydrocarbons, water (H_2O), carbon dioxide (CO_2), carbon monoxide (CO) or similar vaporous products [11]. The processing gas typically flows over the printed parts, transfers the heat and sweeps away decomposition products [12]. Therefore, the condensation of organic residuals can be avoided in the cold regions of the furnace, which reduces the cleaning procedures over time. If the binder can be broken down into gases of low molecular weight such as methane (CH_4), ethane (C_2H_6) or propane (C_3H_8), then they do not condense in the furnace chamber [13]. The decomposition behavior and temperature of the binder are influenced by the surrounding atmosphere, which will be discussed in section 3.2.

2.3 Sintering

In this chapter, the basic principle of sintering is explained. Based on that, common practices, process parameters and challenges of sintering of green parts manufactured via BJT are summarized.

2.3.1 Basic principle of sintering

Sintering can be described as a heat treatment process, where the binding of adjacent metal particles is achieved by atomic diffusion and other mass transport mechanisms at elevated temperatures. The driving force for sintering is the reduction of interfacial energy to reach a thermodynamically more stable condition. A green part contains a high amount of free surface energy compared to a dense bulk material. The minimization of the free surface energy is achieved by diffusion processes between the particles, which can be separated into two aspects. On the one hand, densification transforms solid-gaseous surfaces into solid-solid interfaces decreasing the interfacial energy. On the other hand, interfacial energy is further reduced by grain growth, which decreases the grain boundary surface area [14]. High temperatures are required for sufficient sintering kinetics.

The sintering of two adjacent particles and the different types of mass transport mechanisms are visualized in Figure 4. Bulk and surface transport mechanisms occur during sintering, which both contribute to sintering neck growth. The bulk mass transport relocates mass from the inside of the solids into the pores [12]. Only bulk transport mechanisms induce shrinkage and densification. The repositioning of mass on the pore surface to smooth pores and decrease the surface area does not pull the particles closer together.

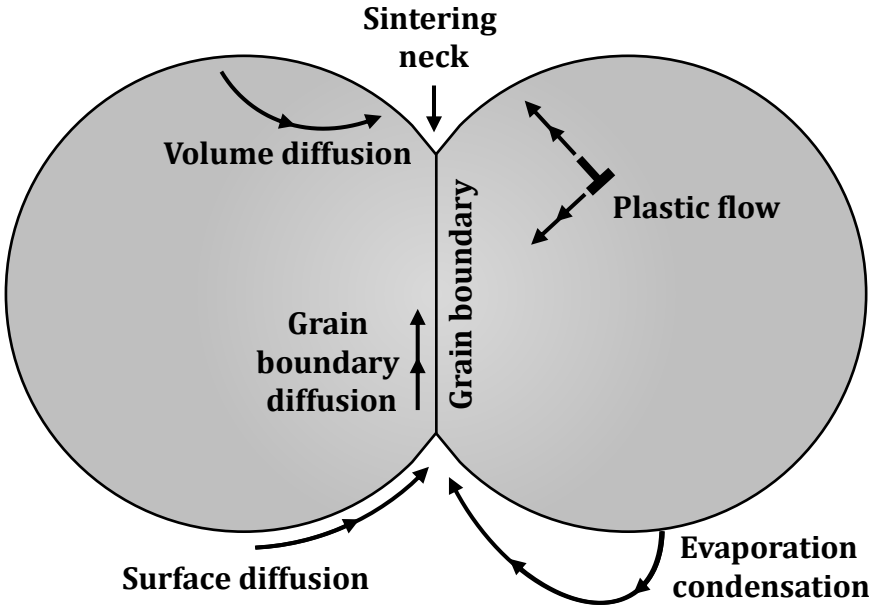

Figure 4: Mass transport mechanisms during sintering of two spherical particles adapted from [14].

For loose powder compacts produced by AM, the sintering process can be classified into four stages [11]. The first stage is the contact formation by the adhesive forces that pull the metal particles together [11]. The initial bonding at the particle contacts through surface diffusion is the second stage of the sintering process, which is called neck growth [11]. During the third stage, the merging of growing necks forms tubular pores leading to pore rounding [11]. The last stage is pore closure, where grain growth with closed porosity occurs [11]. The residual pores collapse into spherical voids that disappear if they are not entrapped with an insoluble gas [11]. The resulting evolution of density and correlated shrinkage during sintering over time is highlighted in Figure 5 for a simple sintering cycle.

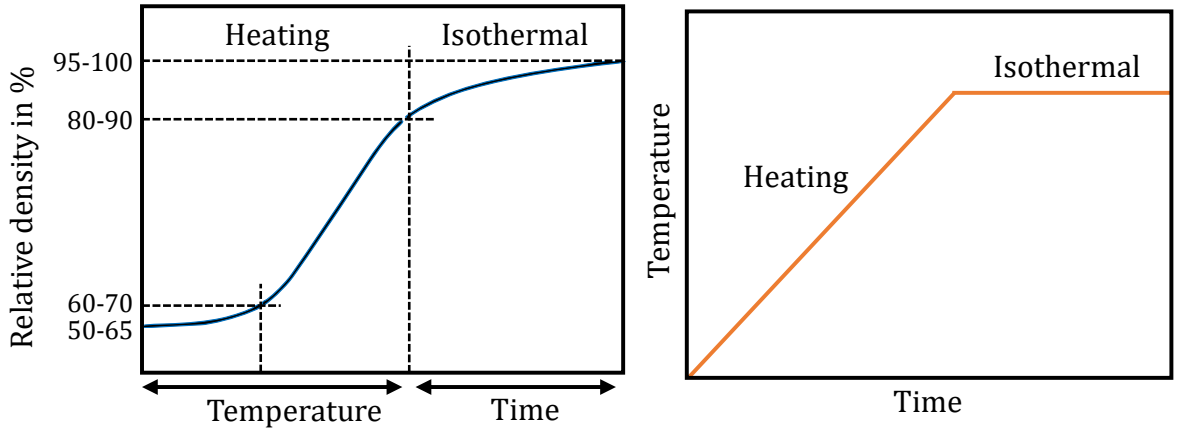

Figure 5: Schematic density evolution during sintering adapted from [15].

Sintering is one of the most critical steps in the process chain of BJT because it determines the part's final dimensions and material properties. Different types of sintering strategies are followed, where the sintering temperature can be close to the melting temperature of the base material. Sintering can be performed below the solidus temperature without forming liquid phases, which is defined as solid-state sintering. Solid-state sintering provides a good balance between high sintered density and moderate shrinkage. In contrast, supersolidus-liquid-phase sintering is sintering above the solidus temperature, where small amounts of liquid phases form [16]. Creating liquid phases during sintering improves the sintering densification, but excessive liquid phases distort the part geometry [17]. Another strategy is infiltrating the porous structure with a lower melting material such as bronze. The approach of infiltration gives the best dimensional accuracy by filling the porosity, but it creates a composite material.

2.3.2 Parameters of the sintering process

Many process parameters impact the sintering densification. Industrial sintering operations are mainly defined by the heating rate, peak temperature, dwell times and the processing atmosphere [11]. The chosen parameters for sintering depend on the powder characteristics, green part properties and the required density after sintering. The most important considerations for sintering include:

- Powder properties:
  - Particle size distribution (PSD)
  - Powder morphology
  - Bulk chemistry
  - Surface chemistry
  - etc.
- Green part characteristics:
  - Density & density gradients
  - Shape
  - Binder content
  - Binder formulation
- Sintering parameters:
  - Peak temperature
  - Heating rate
  - Dwell times
  - Atmosphere

The powder properties influence the sintering activity. Smaller particle sizes are generally favored for high densification [18,19]. The powder's composition, especially its surface state, influences the sintering neck formation. The bulk chemistry determines phase composition and its transformations during the sintering process. Hence, it influences the sintering activity due to changes in diffusion coefficient, phase composition, grain sizes and the forming of new interfaces [11]. A common phase transformation is found in iron from body-centered cubic (bcc) to face-centered cubic (fcc) lattice structure. The bcc crystallographic lattice structure has a higher self-diffusion than the fcc lattice structure [20]. Carbon introduced by a binder can affect the microstructure and phase transformations of stainless steel [21,22].

Green parts manufactured via BJT typically have green densities of ~50 % to ~60 % relative to the bulk material [23]. A higher powder packing is generally favored for sintering densification due to more inter-particle contact points. The properties of a green part inherent to the BJT process need to be taken into account to reach a specified geometry. The layer-wise shaping process leads to higher porosity between two deposited layers compared to the porosity inside a single layer, which manifests in higher shrinkage in the build direction [24,25]. This anisotropy in shrinkage needs to be considered when designing green parts. The anisotropy in densification is the subject of research and sintering simulations. The presence of high and low-density regions inside

a green part causes warping during sintering [12]. The sintering process enhances variations caused by the shaping process [12].

While the design freedom of AM enables the production of complex shapes, shape retention during sintering becomes more challenging. Gravity causes distortion during sintering, especially for unsupported and overhanging features [26,27]. Furthermore, friction between the part and the sintering setter can cause non-uniform shrinkage. Often, sintering supports might be required to counteract these phenomena.

Sintering parameters are set based on the powder characteristics, green part properties and target density. Sintering densification generally increases with higher peak temperatures, while the densification rate slows down with longer dwell times [12]. Most of the sintering happens during heating and not during the holding time at peak temperature [11]. Dwell times at sintering temperature are often applied to ensure full heating of a component. Long dwell times are usually avoided due to grain and pore growth negatively impacting mechanical performance. Rapid heating is also not advisable because of the nonuniform heating of the sample. Common heating rates for sintering are between 5 °C/min and 10 °C/min. The influence of the sintering atmosphere is briefly summarized in section 3.3.

The density after sintering is indicative of the mechanical properties. For most materials, a power law between strength and fractional density is observed, which is formulated according to equation (1). The calculated material strength is σ and the fractional density is f. σ_0 corresponds to the strength at full density.

$$\sigma = \sigma_0 f^N \tag{1}$$

The exponent N is typically between 4 and 6 and is connected to the sensitivity of the material to the remaining porosity [11]. For an exponent N = 4.3, a fractional density of 85 % would correspond to 50 % of the strength of the fully dense material [11].

Post-processing operations can enhance the quality of the part after sintering. Common post-processes are heat treatment, surface finishing, machining or Hot Isostatic Pressing (HIP). The applied post-processes are selected based on the application requirements but increase the manufacturing costs and time. Heat treatments are used to achieve certain microstructures and specific material properties. Surface finishing and machining might be applied to reach tolerances and required surface roughness. HIP is a process to reduce porosity by simultaneously applying heat and pressure to the part to close the residual pores. It is mainly used for high-performance applications that require a high density.

3 Processing atmospheres in Binder Jetting

In this chapter, the role of the processing atmosphere along the different stages of BJT is discussed. While the role of the atmosphere is less critical for printing at room temperature, the role of the atmosphere becomes more critical for the process steps involving thermal treatment.

3.1 Printing, curing & depowdering atmospheres

The BJT printing process is conducted at ambient temperature. Therefore, oxidation during printing is not expected and most systems operate in air. Oxygen in the printing environment can, however, limit the choice of materials for printing due to the explosion risks associated with fine and reactive metal powders such as titanium or aluminum. Printing and depowdering in an inert atmosphere can enhance the material choice. An inert and controlled environment can also be facilitated to ensure a robust process since changes in ambient humidity can affect the powder-spreading behavior. Furthermore, the binder wetting can be influenced by moisture [28]. During the curing process, the powder is subjected to heat. Curing is often performed in air, so the powder is susceptible to oxidation.

3.2 Debinding atmospheres

The atmosphere can have two functions during debinding depending on the composition. First, a constant flow of gas or a vacuum facilitates the removal of debinding products from the part. Second, the debinding atmosphere can provide potential reaction components to enable binder decomposition at elevated temperatures. The choice of atmosphere depends mainly on the binder and furnace equipment.

During debinding, vacuum or protective atmospheres, including Ar and N_2, are commonly used to prevent the oxidation of metal powders [11]. In inert environments, debinding is dominated by pyrolysis. The breakdown comes from the polymer itself since no reactive species is provided by the atmosphere [12]. Using inert debinding atmospheres often results in carbon residuals in the form of graphite [12]. This carbon contamination is not a concern for high-carbon containing materials like tool steels or cemented carbides but can be problematic for stainless steels or other materials such as copper or nickel-base superalloys [12]. Vacuum during debinding can decrease the binder evaporation temperature and aid the binder removal from the part [11]. The binder poses, however, a problem for sensitive vacuum furnace equipment, especially by clogging and damaging vacuum pumps. Hence, debinding in an expensive vacuum sintering furnace might be avoided.

The binder decomposition is altered by reactive species such as O_2, H_2O or hydrogen (H_2), helping to form volatile species [12]. Reactive atmospheres containing O_2 or H_2 accelerate the reaction and allow lower decomposition temperatures compared to inert atmospheres [12]. Common decomposition products formed during debinding are H_2O, CO, CO_2, CH_4 and more complex hydrocarbons depending on the set debinding

temperature [12]. O_2-containing atmospheres during debinding are efficient in removing carbon from the binder, but the powder is more prone to oxidation [12].

3.3 Sintering atmospheres

The composition and purity of the sintering atmosphere have a decisive impact on the sintering result since they strongly affect reactions on the metal powder surfaces [11]. Metal powders form a natural oxide layer at the powder surface in ambient conditions, which hinder sintering neck formation [29]. The surface oxides can be removed by dissociation or reduction reactions during sintering. Potential reducing species for metal oxides are typically hydrogen, carbon or carbon monoxide [30]. The choice of the sintering atmosphere is dependent on the material, the required material properties and the dimensional accuracy [11].

Inert atmospheres are a common choice for sintering to prevent metal oxidation. Furthermore, unwanted reactions caused by the gas such as carburization or decarburization can be avoided. Ar is an insoluble, inert gas that gets entrapped inside the pores during sintering. This entrapment of gas impedes the final stage densification of the pores due to increasing pore pressure countering the sintering stress [11,12]. This is especially critical if HIP is applied for pore closing. N_2, another frequently used inert gas, can cause nitride formation during sintering. Helium (He) can also be used possessing excellent heat transport properties, but it is comparatively expensive.

H_2 is another effective sintering atmosphere due to its reducing capabilities. In addition, H_2 possesses a high thermal conductivity that helps to cause uniform heating [11]. The reduction of metal oxides (M_xO_y) by H_2 is described by equation (2), where H_2O is the reaction product. Mixtures of inert gas and H_2 are also frequently used including Ar-H_2 mixtures and N_2-H_2 mixtures [11]. H_2 is most effective for the removal of surface iron oxide during the early stages of sintering [31].

$$\frac{2}{y}M_xO_y + 2H_2 \leftrightarrow \frac{2x}{y}M + 2H_2O \qquad (2)$$

Reduction reactions during sintering are not limited to H_2. Another common reduction mechanism encountered during sintering is carbothermal reduction. It is distinguished between direct and indirect carbothermal reduction. Direct carbothermal reduction is the reduction of the metal oxide by carbon forming CO, which is defined by equation (3). The indirect carbothermal reduction is the reduction of the metal oxide by CO with CO_2 as the reaction product provided by equation (4). The direct and indirect carbothermal reductions are determined by the Boudouard equilibrium given by equation (5). The formation of CO is thermodynamically favored above 720 °C. While elemental carbon can originate from the binder or powder, CO can be provided by a sintering gas or be formed as a reaction product during sintering.

$$\frac{2}{y}M_xO_y + 2C \leftrightarrow \frac{2x}{y}M + 2CO \quad (3)$$

$$\frac{2}{y}M_xO_y + 2CO \leftrightarrow \frac{2x}{y}M + 2CO_2 \quad (4)$$

$$C + CO_2 \leftrightarrow 2CO \quad (5)$$

Vacuum is also frequently used to achieve low O_2 partial pressures during sintering. Low O_2 partial pressures can provide conditions suitable for the dissociation of metal oxides at the sintering temperature but this strongly depends on the stability of the oxide. The dissociation of metal oxides can be universally described by equation (6).

$$\frac{2}{y}M_xO_y \leftrightarrow \frac{2x}{y}M + O_2 \quad (6)$$

Below 500 °C, heat transfer is primarily achieved via the atmosphere, which benefits from a high thermal conductivity gas [32]. Vacuum is not favorable for low sintering temperatures. At higher temperatures, radiation is the dominating mechanism of heat transfer [32,33].

4 Experimental Methods

In this chapter, the materials and methods used in this thesis study are briefly summarized. First, the raw materials and the printing process are described. Then, the experimental methodology for the reusability study and the debinding experiments is introduced. Last, the analytical techniques for powder and material characterization are listed.

4.1 Materials & printing process

This work used N_2-atomized pre-alloyed 17-4 PH stainless steel powder (Desktop Metal Inc., USA) as the raw material. The powder was conditioned by oxidation to reach certain flowability characteristics for printing. A water-based binder (SPJ-04, Desktop Metal Inc., USA) was applied for printing. Besides water, the binder contained solvents and a thermoset polymer.

A Production System P1 (Desktop Metal Inc., USA) was employed for BJT printing. The used layer thickness was 65 µm. The printer includes O_2 and humidity control sensors and gas purging of the build chamber. In contrast to most BJT hardware, the system functioned with a carriage moving the build box instead of moving the printhead and powder spreading units. Furthermore, a steamer was employed to apply steam on each deposited layer before binder deposition to prevent powder ejecta during printing, which can clog the printhead nozzles. A powder layer was deposited and printed in a single pass of the build box. This resulted in a processing time as low as 5 seconds per layer.

The build box was cured after printing in a forced air-convection furnace (TR 120 LS, Nabertherm GmbH, Germany). A heating rate of 1.5 °C/min to a maximum temperature of 200 °C was applied and a dwell time of 4 h was set. Natural cooling of the furnace was taking place after the dwell time. After curing, the green samples were separated from the loose powder bed inside an inert environment with tools such as brushes and tweezers. After rough depowdering with tools, compressed air or gas was used to get rid of the remaining powder.

4.2 Study on the reusability of 17-4 PH stainless steel powder

To study the impact of powder reuse on powder characteristics and print results in Paper I, 30 kg of 17-4 PH virgin powder was introduced for continuous reuse. The powder was reused for a total of 20 build jobs. Cuboid specimens with dimensions of 10 x 10 x 10 mm^3 were used for comparison of each build job. The powder to analyze was differentiated into overflow powder and depowdered powder. The overflow powder was oversupplied powder directly reused in the printer. Five consecutive build jobs were conducted by directly reusing the overflow powder generated during printing. Those five build boxes were placed together into the curing furnace. After curing, the powder from the depowdering step was sieved and used to conduct the next five consecutive build jobs. This cycle was conducted a total of four times resulting in a total of 20 build jobs.

The influence of powder reuse on print quality was assessed by green density and part accuracy. The change in powder characteristics over 20 build jobs was closely monitored through the bulk oxygen content, humidity, PSD and flowability measurements. More detail is provided in section 4.4. To investigate the impact of curing on the powder in an inert and slightly reducing environment, the unprocessed 17-4 PH virgin powder was subjected to 200 °C for 4 h in air, Ar and a forming gas mixture with 95 vol.% N_2 and 5 vol.% H_2.

4.3 Study on debinding atmosphere compositions for 17-4 PH

The influence of oxygen content in the debinding atmosphere during debinding of 17-4 PH green parts was investigated in Papers II and III. Cuboid samples with dimensions of 10 x 10 x 10 mm^3 and additional cylinders with a diameter of 2.9 mm and a height of 11.9 mm were printed. The latter were solely used for elemental analysis. The obtained samples were debinded and sintered in a laboratory tube furnace with a steel muffle tube. The gas flow for debinding and sintering was constant for all gases at 4 l/min. The temperature close to the samples was measured via a thermocouple inside the tube to ensure comparable temperatures. The oxygen content at the furnace outlet was tracked via an oxygen monitoring device (Hydroflex, Linde GmbH, Germany) to verify a high-purity atmosphere.

The debinding process in Paper II was operated at 300 °C for 2 h. The heating rate was 1.5 °C/min. The debinding atmospheres investigated included inert Ar, Ar + 1 vol.% O_2, Ar + 3 vol.% O_2, Ar + 4 vol.% O_2 + 5 vol.% CO_2, Ar + 8 vol.% O_2 and N_2 + 20 vol.% O_2. The debinding results were assessed by density, weight loss and part chemistry. The impact of the debinding atmosphere on the sintered samples was examined in Paper III. All sintering operations of the obtained brown parts were performed at a peak temperature of 1300 °C with a dwell time of 2 h in an inert Ar atmosphere. Ar was chosen to avoid any reactive species provided by the sintering atmosphere. The cooling of the furnace took place under a constant gas stream. The sintered samples were analyzed by density, shrinkage, microstructure and chemistry described in section 4.4. Furthermore, Thermo-Calc software (Thermo-Calc Software AB, Sweden) was used to predict phases present during sintering by thermodynamic calculations.

4.4 Analytical techniques

The analytical techniques used to analyze the powder, green parts, brown parts and sintered parts are described in this section. The same characterization methods were applied for Papers I, II and III.

4.4.1 Powder characterization

The 17-4 PH powder was characterized by different techniques to assess the impact of powder characteristics on the printing and sintering process. The elemental composition of the 17-4 PH virgin powder was measured by inductively coupled plasma optical emission spectroscopy (ICP-OES) and X-ray fluorescence spectroscopy (XRF).

The PSD was evaluated through a dynamic imaging technique (CAMSIZER® X2, Microtrac Retsch GmbH, Germany). The humidity contents were determined via Karl Fischer titration (C30S Compact KF Coulometer, Mettler-Toledo GmbH, Germany). Dynamic flow analysis (Revolution Powder Analyzer 2015, Mercury Scientific Inc., USA) was utilized to investigate the flowability with 100 ml of powder at 0.6 rpm.

4.4.2 Elemental analysis

The oxygen, nitrogen and hydrogen contentrations of the 17-4 PH powder, green parts, brown parts and sintered samples were determined via the inert gas fusion method (ONH836, LECO Corporation, USA). For carbon analysis of the listed samples, the inert gas fusion technique (CS 2000, ELTRA GmbH, Germany) was also utilized.

4.4.3 Density & shrinkage analysis

Three different methods for the density determination of samples were used. The volumetric density was calculated for green parts and sintered parts via the weight and volume. The weight was measured with a precision scale (QUINTIX224-S1, Sartorius AG, Germany). The volume was calculated by measuring the dimensions with a manual micrometer screw gauge. The dimensions after sintering were determined to calculate the shrinkage in X-, Y- and Z-direction. For sintered samples, the Archimedes' principle was utilized as a second method to determine the density. The third method was porosity analysis by microscopy, which is described in the following section.

4.4.4 Microstructural investigation

After sintering, the cuboid specimens were cut in half two times to have two perpendicular cross-sections to analyze. The cut halves were hot-embedded, ground and polished. The metallographically prepared samples were analyzed by light optical microscopy (VHX-6000, Keyence, Germany). The areal density of ground and polished cross-sections was determined via the thresholding method using the image analysis software Fiji (open-source). After the porosity was determined, the samples were etched using Kalling's reagent to reveal microstructural features by light optical microscopy.

5 Summary of appended papers

This section summarizes the appended papers to answer the previously formulated research questions. The first research question is addressed by Paper I, where 17-4 PH stainless steel powder was reused over 20 build jobs. The second research question is answered in the manuscripts of Paper II and Paper III, where the influence of decreasing oxygen contents in the debinding gas for 17-4 PH was analyzed. A particular focus was placed on the chemical evolution from virgin powder to sintered parts.

5.1 Reusability of 17-4 PH stainless steel powder in BJT

Paper I aimed to understand if the continuous reuse of 17-4 PH powder affects the powder characteristics and changes the printing behavior. Therefore, the same powder was reused for 20 consecutive build jobs under constant processing conditions. Furthermore, virgin powder was conditioned at 200 °C for 4 h in different atmospheres to see the impact of the curing atmosphere on powder oxidation.

5.1.1 Print quality & accuracy

The influence of powder reuse on green densities is shown in Figure 6. Note that the green densities from build job 11 were excluded due to a print error. Comparable green densities were found for the first five consecutive build jobs reusing the overflow powder from the previous build job. After a curing and sieving step, a considerable decrease of ~0.11 g/cm^3 in green densities was measured for build job six. This decrease was linked to a lower powder packing in the powder bed since the binder makes up only ~1 wt.% of the green part.

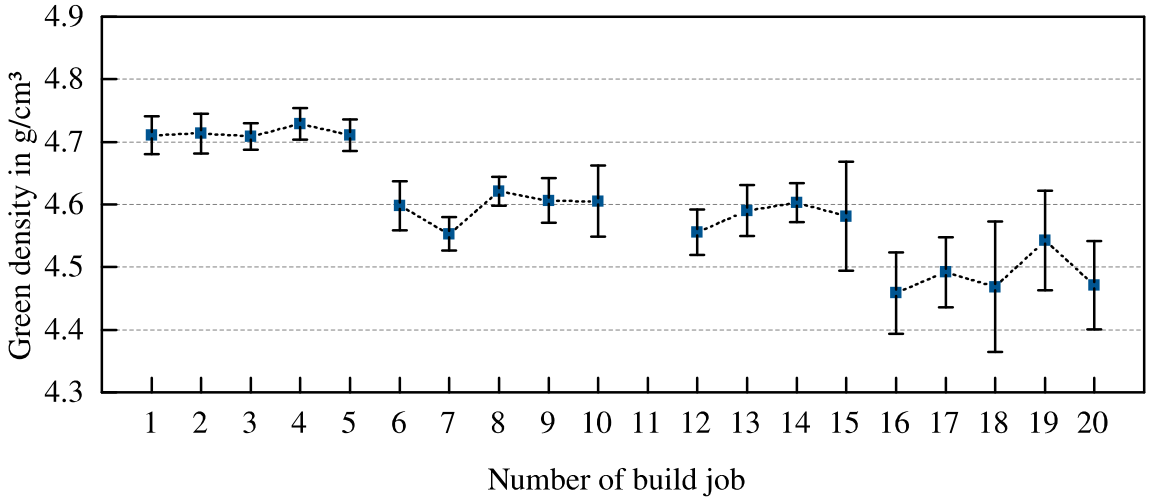

Figure 6: Green part densities for reusing 17-4 PH powder over 20 build jobs.

Over 20 build jobs, the average green densities decreased from 4.71 ± 0.03 g/cm^3 in the first build job to 4.47 ± 0.07 g/cm^3 in the last build job. The accuracy was nearly unaffected for 15 build jobs, while the build jobs 16 to 20 showed increasing dimensional errors. In general, the accuracy in the build direction was the highest. Reusing oversupplied powder for five times did not affect the green densities and print accuracy.

5.1.2 Powder degradation

The powder characteristics were analyzed after each build job separated into oversupplied powder (overflow powder), powder taken from the depowdering step (depowdered powder) and the subsequent sieved powder after depowdering (R1-R4). For the first five build jobs, no noticeable change in powder characteristics such as PSD, oxygen content and humidity was measured. Consequently, comparable green densities and dimensional accuracy were obtained for the first five build jobs.

The evolution of the oxygen content over the 20 build jobs for the different types of powder is highlighted in Figure 7. A significant increase in bulk oxygen content by ~15 % of the 17-4 PH powder was revealed in the samples taken from depowdering of the first five build jobs. The oxygen pickup was caused by the O_2 present in the ambient air during curing at 200 °C for 4 h. The increase in oxygen correlated with the decrease in green densities. The powder was subjected in total to four curing cycles for the 20 build jobs. The bulk oxygen content increased overall from 1200 ppm in the virgin powder (V) to 1443 ppm in the sieved powder after 20 build jobs (R4).

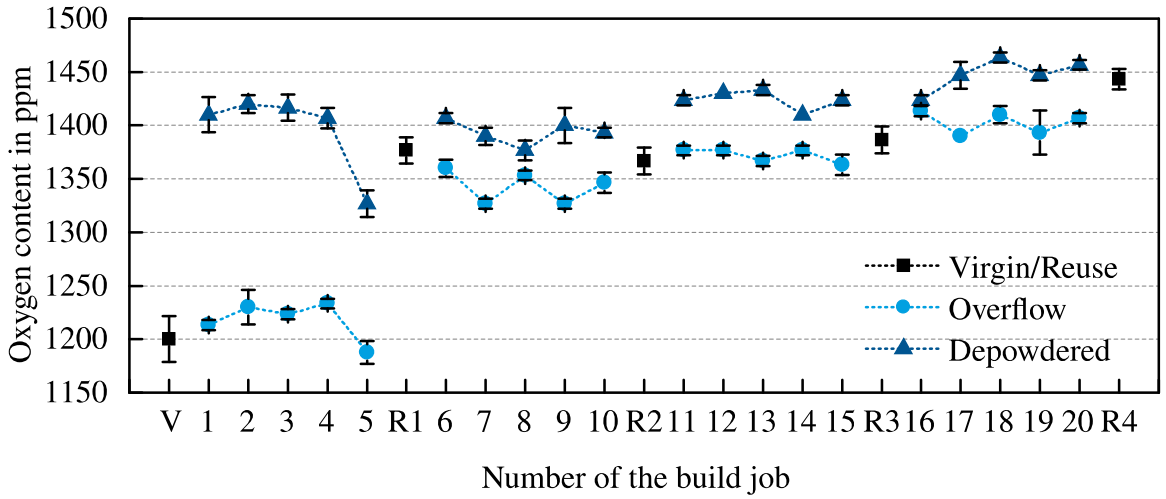

Figure 7: Total oxygen content of 17-4 PH stainless steel powder reused over 20 build jobs. R1 to R4 corresponded to the powder after curing and sieving.

The humidity contents of powders showed no clear trend. A slight increase was indicated between build jobs five and six, which remained at a comparable level until build job 20. Flowability values showed a slight difference after 20 build jobs. The PSD shifted slightly to higher average diameters over 20 build jobs. The median particle size (D_{50}) increased by ~1 µm. The measurement of very fine powder was, however, limited by dynamic image processing. The increase in PSD can be a reason for the decrease in green density. Loss of fine powder particles due to powder handling was likely since the fine fractions are easily air-born or stick to surfaces. It is unclear whether the slight coarsening of the PSD or the oxygen uptake was responsible for the decrease in green density. A combination of both is likely.

5.1.3 Powder conditioning

17-4 PH powder subjected to thermal treatment at 200 °C for 4 h revealed the same oxidation as the powder taken from the build box after curing. The use of an inert or slightly reducing atmosphere prohibited oxidation of the powder conditioned at 200 °C for 4 h. Powder oxidation during curing needs to be prohibited to keep the powder characteristics and printing results constant. Furthermore, increased surface oxidation of the powder can pose challenges for subsequent sintering of green parts, as surface oxides must be removed for sintering neck formation.

5.2 Influence of oxygen content in the debinding atmosphere on debinding and sintering of BJT processed 17-4 PH stainless steel

Paper II and Paper III examined the impact of different oxygen content in the debinding atmosphere on 17-4 PH green samples. The focus of the research was to understand how the chemistry of the 17-4 PH powder changed from green part to brown part and finally to sintered part. The results were correlated with the final densities and microstructures.

5.2.1 Impact of oxygen content in the debinding atmosphere on brown parts

The binder content in a green sample was calculated to be ~1.5 wt.% before curing and ~1.0 wt.% after the curing process. The curing process removed mainly oxygen, hydrogen and nitrogen. This was attributed to water and solvent evaporation. After the curing process, the binder added roughly 0.56 wt.% of carbon, 0.38 wt.% of oxygen, 0.05 wt.% of hydrogen and 0.02 wt.% of nitrogen relative to the 17-PH virgin powder. The binder added approximately 0.05 g/cm^3 to the density of the green part, which depends on the set binder saturation.

The debinding of green parts in inert Ar yielded a low debinding efficiency at 300 °C for 2 h, as ~34 % of the binder was removed leaving high amount of carbon-rich residues in the brown part. Adding 1 vol.% O_2 to the debinding atmosphere increased the binder removal to ~74 % of the initial binder mass. The binder was almost completely removed after debinding in processing gas compositions containing 3 vol.% O_2 to 20 vol.% O_2, which resulted in minor powder losses due to increased brown part brittleness. The part weight losses matched in general the binder contents determined by the brown part chemistry. The 17-4 PH powder picked up 1734 ppm to 1820 ppm of oxygen when debinded in 3 vol.% O_2 to 20 vol.% O_2. Slightly lower oxidation of the loose powder at 300 °C was measured in Ar + 1 vol.% O_2 with an increase of 1617 ppm, while only 60 ppm of oxygen was picked up for conditioning the powder in inert Ar.

5.2.2 Impact of oxygen content in the debinding atmosphere on sintered parts

The final oxygen and carbon levels after sintering are shown in Figure 8. The brown parts debinded in Ar revealed nearly complete oxygen removal from 1163 ppm in the virgin powder to 19 ppm in the material after sintering. Excessive carbon pick-up was, however, found after sintering. The cause of deoxidation was carbothermal reduction by carbon originating from the binder since no reducing species were provided by the sintering atmosphere.

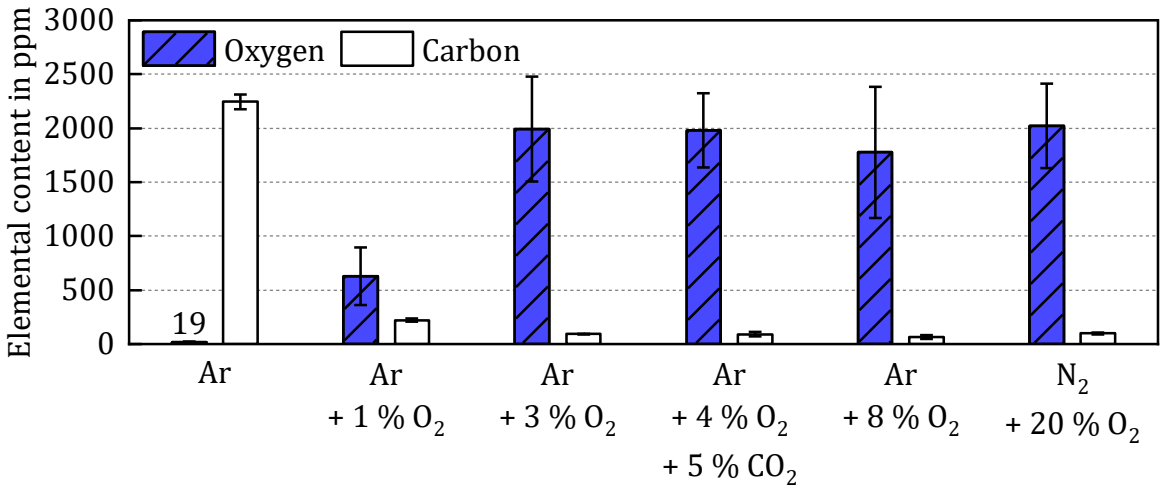

Figure 8: Oxygen and carbon levels of sintered parts debinded at 300 °C for 2 h in atmospheres with various oxygen contents.

Brown samples debinded in Ar + 1 vol.% O_2 exhibited a carbon content similar to the virgin powder after sintering, but the final oxygen content decreased by 46 % relative to the virgin powder. This indicates that carbothermal reactions caused oxygen reduction, but binder contamination was avoided at the same time. Less carbon was in the brown part compared to debinding in Ar. Brown parts debinded in processing gas containing 3 vol.% O_2 to 20 vol.% O_2 showed deoxidation after sintering, but the final oxygen content was 53 % to 74 % higher than in the virgin powder. The oxidation induced during debinding could not be completely reversed by carbothermal reduction as the binder content in the brown parts was low. The results demonstrated that a moderate amount of binder in the brown part can be beneficial for deoxidation during sintering.

The influence of the carbon content on the sintering activity of 17-4 PH was indicated by the densification after sintering. Debinding in Ar resulted in densities of ~88 % after sintering, whereas debinding in Ar + 1 vol.% O_2 achieved densities of ~98 %. The debinding in processing gas containing 3 vol.% O_2 to 20 vol.% O_2 resulted in comparable densities of ~96 % to ~98 % after sintering. The microstructures revealed the reason for the difference in sintering densification, which is displayed in Figure 9 for debinding in Ar, Ar + 1 vol.% O_2 and N_2 + 20 vol.% O_2.

Debinding in oxygen-containing atmospheres revealed δ-ferrite distributed along prior austenite grain boundaries in contrast to samples debinded in Ar, where no δ-ferrite phase could be identified in the microstructure. δ-ferrite promotes the sintering activity as the volume diffusion in the bcc lattice structure of the δ-ferrite phase is one to two orders higher than in the fcc lattice of the γ-austenite phase [34]. The absence of δ-ferrite was caused by the high carbon content of 0.22 wt.% after sintering since carbon is a strong austenite stabilizer. This was in accordance with thermodynamic equilibrium calculations that predicted no δ-ferrite present at 1300 °C for carbon contents above 0.16 wt.%.

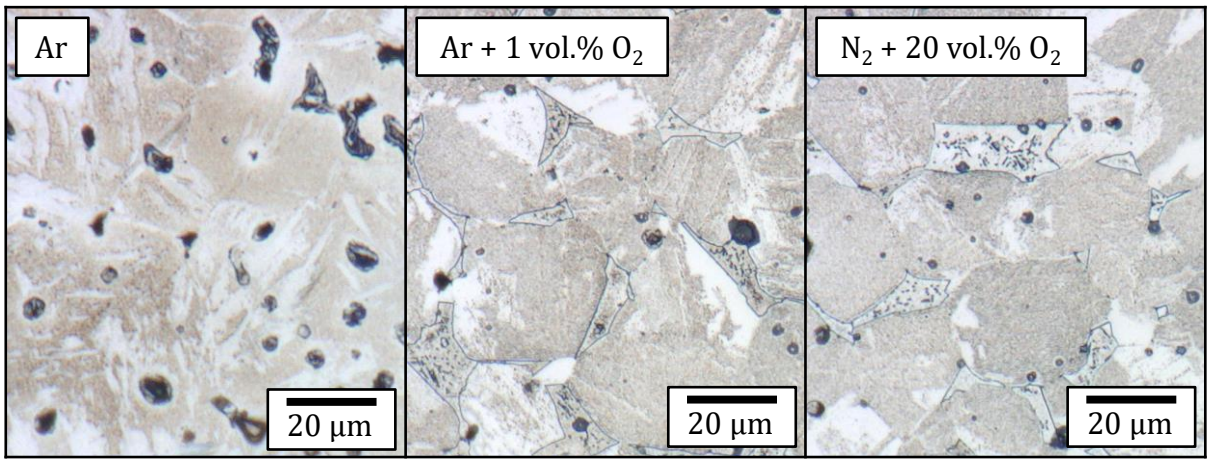

Figure 9: Etched microstructures of 17-4 PH after sintering for debinding at 300 °C for 2 h in inert Ar, Ar + 1 vol.% O_2 and N_2 + 20 vol.% O_2.

It was shown that excessive amounts of carbon hinder the formation of δ-ferrite, which is important for the densification of 17-4 PH during sintering. At the same time, carbon efficiently reduces metal oxides in the powder alloy. Debinding in Ar + 1 vol.% O_2 achieved the best combination of high densification, oxide reduction and no carbon pick-up during sintering.

6 Summary and Conclusions

This thesis investigated the influence of the processing atmosphere on BJT of 17-4 PH stainless steel. The first part assessed the reusability of 17-4 PH powder over 20 build jobs and the impact of curing atmospheres. The second part investigated the effect of decreasing oxygen contents in the debinding atmosphere on sintering densification and material chemistry of 17-4 PH. The debinding trials with different oxygen content in the atmosphere were conducted at 300 °C for 2 h. Subsequent sintering was performed at 1300 °C in an inert Ar atmosphere.

1. RQ: What is the influence of curing in ambient air on powder degradation and printing repeatability during BJT of 17-4 PH stainless steel?

The reuse of 17-4 PH powder over 20 build jobs decreased green densities from 4.71 g/cm^3 to 4.47 g/cm^3, which indicated a lower powder packing. The decrease in green densities directly correlated with powder oxidation caused by curing in ambient air. The first curing step resulted in the powder's biggest oxygen increase of ~15 %. After 20 build jobs, a slight increase of the PSD was measured by ~1 µm (D_{50}), which might also contribute to lower green densities. Curing in inert atmospheres was concluded as necessary to maintain consistent powder characteristics for a robust BJT process.

2. RQ: What is the impact of decreasing oxygen in the processing atmosphere during debinding on 17-4 PH green part properties, sintering densification and material chemistry?

The binder made up ~1 wt.% of the green part. Debinding in Ar yielded the lowest debinding efficiency introducing high carbon residues after sintering. The high carbon content resulted in nearly complete oxygen removal after sintering by carbothermal reduction. Debinding in Ar + 1 vol.% O_2 removed ~74 % of the initial binder in the green part. Debinding in Ar + 3 vol.% O_2 up to N_2 + 20 vol.% O_2 resulted in almost complete binder removal combined with minor powder losses during handling due to higher brown part brittleness. A decrease of bulk oxygen from brown to sintered sample was measured for all debinding atmospheres. Debinding in Ar + 1 vol.% O_2 resulted in an oxygen reduction of 46 % relative to the virgin powder, whereas debinding in Ar + 3 vol.% O_2 up to N_2 + 20 vol.% O_2 led to an oxygen increase of up to ~74 %. Therefore, the remaining carbon in the brown part was insufficient to reverse the oxidation induced during debinding at 300 °C.

The lowest densities of ~88 % after sintering were obtained for debinding in Ar. The excessive carbon content after debinding in Ar prohibited the formation of δ-ferrite during sintering. The δ-ferrite phase promotes sintering activity due to the higher self-diffusivity compared to the γ-austenite phase. Debinding in oxygen-containing atmospheres achieved comparable densities of 96 % to 98 % due to the nucleation of δ-ferrite along prior austenite grain boundaries. In conclusion, debinding in Ar + 1 vol.% O_2 achieved the best balance of high densification, oxide reduction and no carbon residues after sintering of 17-4 PH.

7 Future work

The first part of this thesis on powder reusability revealed powder degradation resulting in lower green densities when keeping the printing parameters constant. The impact of the different green densities on the sintering densification needs to be assessed. A detailed investigation should be provided using dilatometric analysis and porosity characterization. Furthermore, the change in powder characteristics needs to be further studied by utilizing techniques such as scanning electron microscopy (SEM) and X-ray photoelectron spectroscopy (XPS).

In the second part of this work, the tailoring of the oxygen content in the debinding atmosphere showed a positive effect on the material chemistry of 17-4 PH. A deeper understanding of binder removal and powder oxidation needs to be established by thermogravimetric analysis (TGA) depending on the debinding atmosphere. The influence on the mechanical performance should be investigated, and the correlation to the microstructures, fracture surfaces and material chemistry should be provided. In addition, the effect of the debinding atmosphere on sintering evolution should be investigated by dilatometry.

Sintering in this work was conducted in inert Ar. The comparison of different sintering atmospheres in combination with an improved debinding atmosphere should be investigated. This can provide different routes for debinding and sintering tailored to the constraints and requirements of end-users. Sintering atmospheres of interest include hydrogen, slightly reducing atmospheres and vacuum.

8 Acknowledgments

First of all, I want to thank Pierre Forêt and Eduard Hryha for giving me the chance to pursue a PhD degree in a unique industrial setting on an exciting research topic. While I had the great opportunity to set up a Binder Jetting operation at Linde GmbH in Munich under the industrial supervision of Pierre Forêt, I had the academic supervision of Professor Eduard Hryha from Chalmers University of Technology.

I want to thank my current and former office and PhD colleagues, Tobias Deckers, Julian Henrichs and Siegfried Bähr for their support, valuable feedback and making work more fun, especially when faced with typical research challenges. Furthermore, I want to thank Dr. Elena Bernardo who strongly supported my BJT research at Linde and contributed to great scientific discussions. In addition, I want to thank my current and former colleagues at Linde: Dominik, Tanja, Thomas, Sophie and Ron. I also valued the network that the CAM^2 from Chalmers provided and the PhD students at the IMS that I got to know: Alberto, Anok, Bala, Bharat, Fardan, Laura, Rasmus, Sofia and William.

I am also very grateful to have had the support of great students and interns at Linde who contributed to this work. Special thanks to my two master's thesis students Sankhya Bhattacharya and Mumtahena Jim who carried out a considerable part of the experiments. Furthermore, I want to thank our interns Victor Okafor, Ning Zhang and Fawas Moolakadath. Last, but not least, I want to thank my family and friends who encouraged me during the first part of my PhD degree journey and showed understanding during this busy time in my life.

9 References

[1] Mobarak MH, Islam MdA, Hossain N, Al Mahmud MdZ, Rayhan MdT, Nishi NJ, et al. Recent advances of additive manufacturing in implant fabrication – A review. Appl Surf Sci Adv 2023;18:100462. https://doi.org/10.1016/j.apsadv.2023.100462.

[2] Alami AH, Ghani Olabi A, Alashkar A, Alasad S, Aljaghoub H, Rezk H, et al. Additive manufacturing in the aerospace and automotive industries: Recent trends and role in achieving sustainable development goals. Ain Shams Eng J 2023;14:102516. https://doi.org/10.1016/j.asej.2023.102516.

[3] Zhao N, Parthasarathy M, Patil S, Coates D, Myers K, Zhu H, et al. Direct additive manufacturing of metal parts for automotive applications. J Manuf Syst 2023;68:368–75. https://doi.org/10.1016/j.jmsy.2023.04.008.

[4] Fidan I, Huseynov O, Ali MA, Alkunte S, Rajeshirke M, Gupta A, et al. Recent Inventions in Additive Manufacturing: Holistic Review. Inventions 2023;8:103. https://doi.org/10.3390/inventions8040103.

[5] Mostafaei A, Elliott AM, Barnes JE, Li F, Tan W, Cramer CL, et al. Binder jet 3D printing—Process parameters, materials, properties, modeling, and challenges. Prog Mater Sci 2021;119:100707. https://doi.org/10.1016/j.pmatsci.2020.100707.

[6] ISO/ASTM 52900:2021 Additive manufacturing – General principles – Fundamentals and vocabulary 2021.

[7] 17-4 PH stainless steel: A guide to debinding and sintering for MIM-like Additive Manufacturing processes published. Met Addit Manuf 2018. https://www.metal-am.com/17-4-ph-stainless-steel-a-guide-to-debinding-and-sintering-for-mim-like-additive-manufacturing-processes-published/ (accessed January 12, 2022).

[8] Yu K, Ye S, Mo W, Lv Y, Jiang H, Ma R, et al. Oxygen content control in metal injection molding of 316L austenitic stainless steel using water atomized powder. J Manuf Process 2020;50:498–509. https://doi.org/10.1016/j.jmapro.2019.12.038.

[9] German RM, Bose A, editors. Opportunities for Powder-Binder Forming Technologies. Bind. Polym. Assist. Powder Process., ASM International; 2020, p. 0. https://doi.org/10.31399/asm.tb.bpapp.t59290251.

[10] Forcellese P, Mancia T, Simoncini M, Bellezze T. Investigation on Corrosion Resistance Properties of 17-4 PH Bound Metal Deposition As-Sintered Specimens with Different Build-Up Orientations. Metals 2022;12:588. https://doi.org/10.3390/met12040588.

[11] German R. Thinking about metal Binder Jetting or FFF? Here is (almost) everything you need to know about sintering. Met AM 2019;5.

[12] German RM, Bose A. Binder and Polymer Assisted Powder Processing. ASM International; 2020. https://doi.org/10.31399/asm.tb.bpapp.9781627083195.

[13] Schroeder R, Hammes G, Binder C, Klein AN. Plasma debinding and sintering of metal injection moulded 17-4PH stainless steel. Mater Res 2011;14:564–8. https://doi.org/10.1590/S1516-14392011005000082.

[14] German RM. Coarsening in Sintering: Grain Shape Distribution, Grain Size Distribution, and Grain Growth Kinetics in Solid-Pore Systems. Crit Rev Solid State Mater Sci 2010;35:263–305. https://doi.org/10.1080/10408436.2010.525197.

[15] Salmang H, Scholze H, Telle R, editors. Sintern. Keramik, Berlin, Heidelberg: Springer; 2007, p. 313–80. https://doi.org/10.1007/978-3-540-49469-0_4.

[16] German RM. Supersolidus liquid-phase sintering of prealloyed powders. Metall Mater Trans A 1997;28:1553–67. https://doi.org/10.1007/s11661-997-0217-0.

[17] German RM, Suri P, Park SJ. Review: liquid phase sintering. J Mater Sci 2009;44:1–39. https://doi.org/10.1007/s10853-008-3008-0.

[18] Bai Y, Wagner G, Williams CB. Effect of Particle Size Distribution on Powder Packing and Sintering in Binder Jetting Additive Manufacturing of Metals. J Manuf Sci Eng 2017;139. https://doi.org/10.1115/1.4036640.

[19] Miyanaji H, Rahman KM, Da M, Williams CB. Effect of fine powder particles on quality of binder jetting parts. Addit Manuf 2020;36:101587. https://doi.org/10.1016/j.addma.2020.101587.

[20] Hosford WF, editor. Diffusion. Iron Steel, Cambridge: Cambridge University Press; 2012, p. 98–103. https://doi.org/10.1017/CBO9781139086233.011.

[21] Lecis N, Beltrami R, Mariani M. Binder jetting 3D printing of 316 stainless steel: influence of process parameters on microstructural and mechanical properties. Sci Pap 2021:11.

[22] Wu Y, Blaine D, Marx B, Schlaefer C. Effects of residual carbon content on sintering shrinkage, microstructure and mechanical properties of injection molded 17-4 PH stainless steel. J Mater Sci 2002;37:3573–83. https://doi.org/10.1023/A:1016532418920.

[23] Mirzababaei S, Pasebani S. A Review on Binder Jet Additive Manufacturing of 316L Stainless Steel. J Manuf Mater Process 2019;3:82. https://doi.org/10.3390/jmmp3030082.

[24] Cabo Rios A, Hryha E, Olevsky E, Harlin P. Sintering anisotropy of binder jetted 316L stainless steel: part I – sintering anisotropy. Powder Metall 2021:1–10. https://doi.org/10.1080/00325899.2021.2020485.

[25] Cabo Rios A, Hryha E, Olevsky E, Harlin P. Sintering anisotropy of binder jetted 316L stainless steel: part II – microstructure evolution during sintering. Powder Metall 2022:1–13. https://doi.org/10.1080/00325899.2021.2020486.

[26] German RM, Torresani E, Olevsky EA. Gravity-Induced Distortion During Liquid-Phase Sintering. Metall Mater Trans A 2023;54:4141–50. https://doi.org/10.1007/s11661-023-07078-w.

[27] Torresani E, German RM, Huff R, Olevsky EA. Influence of gravity on sintering of 3D-printed powder components. J Am Ceram Soc 2022;105:131–46. https://doi.org/10.1111/jace.18056.

[28] Inkley CG, Lawrence JE, Crane NB. Impact of controlled prewetting on part formation in binder jet additive manufacturing. Addit Manuf 2023;72:103619. https://doi.org/10.1016/j.addma.2023.103619.

[29] Munir ZA. Surface Oxides and Sintering of Metals. Powder Metall 1981;24:177–80. https://doi.org/10.1179/pom.1981.24.4.177.

[30] Kareem MQ, Mikó T, Gergely G, Gácsi Z. A review on the production of 17-4PH parts using press and sinter technology. Sci Prog n.d.

[31] Hryha E, Nyborg L. Thermogravimetry study of the effectiveness of different reducing agents during sintering of Cr-prealloyed PM steels. J Therm Anal Calorim 2014;118:825–34. https://doi.org/10.1007/s10973-014-3915-z.

[32] German RM. Chapter Fifteen - Sintering Practice. In: German RM, editor. Sinter. Empir. Obs. Sci. Princ., Boston: Butterworth-Heinemann; 2014, p. 471–512. https://doi.org/10.1016/B978-0-12-401682-8.00015-X.

[33] Murashov VV, White MA. Thermal conductivity of crystalline particulate materials n.d.

[34] Wu Y, Blaine D, Schlaefer C, Marx B, German RM. Sintering densification and microstructural evolution of injection molding grade 17-4 PH stainless steel powder. Metall Mater Trans A 2002;33:2185–94. https://doi.org/10.1007/s11661-002-0050-4.